AXIAL CRUSHING OF FIBER FILLED THIN TUBES

AMZATUL AKMAM MOKHTAR
PROFESOR MADYA DR. MD. RADZAI SAID

Paper Presented at the Prosiding Seminar Pencapaian Penyelidikan KUTKM (REACH 2006)
18 – 20 Disember 2006, Holiday Inn Resort, Batu Feringgi, Pulau Pinang

UNIVERSITI TEKNIKAL MALAYSIA MELAKA

Axial Crushing of Fiber Filled Thin Tubes

Amzatul Akmam Bin Mokhtar
Assoc. Prof. Dr. Md. Radzai Bin Said

Faculty of Mechanical Engineering
(KUTKM)

ABSTRACT

The energy absorption capacity of a series of axially crushed tubes filled with oil palm fiber is compared with empty tube. This is to determine the viability of considering the use of such composites or bimaterials in transportation system especially in automotive application. The cross-sectional of tubes are square and rectangular in shape. The tubes are filled with Empty Fruit Bunch (EFB) fibers and with Oil Palm Frond (OPF) fibers; and some of them were added with water or urea formaldehyde. The fibers densities are ranging from 150 kgm^{-3} to 300 kgm^{-3}. It was also found that the rectangular mild steel tubes filled with 300 kgm^{-3} Oil Palm Frond fiber was good in absorbing energy compared with others densities.

KEYWORDS

Energy absorption, transportation, quasi-static, fiber

1. INTRODUCTION

The study of energy absorption is important to the design of safe, crashworthy vehicles [1-4]. When a vehicle is involved in a crash, the kinetic energy of a vehicle must be controlled in such a manner as to prevent injurious loading to the occupants. The energy can be controlled by using either an active or a passive energy management system. An example of an active system for aircraft is the ballistic parachute in which a parachute is fired out of the fuselage and slows the aircraft. Crushable floors and nose cones are also used in aircraft; these devices are considered passive energy absorbers. In the automotive industry, airbags are the most common form of active energy management systems used.

One of the current design theories for passenger vehicles is to have a progressively compliant front end and a rigid passenger compartment. A progressively compliant front end consists of a series of 'crumple zones' each resisting deflection until a certain load level is reached, and then deforming at that constant load level until the next zone is reached. The first zone deforms at a very low load level to protect pedestrian and cyclists. The series of zones that follow are designed for increasing level of load; the final zone is rigid passenger compartment which should resist all deflection.

When studying energy absorption there are many important variables. These include materials; manufacturing methods, microstructure, geometry of specimen, including any crush initiator used; and rate of crush. An important parameter when studying energy absorption, and one often used in the automotive industry, is the energy absorbed per unit mass of crushed material. This is often called the specific energy absorption (SEA). The SEA provides a measure of energy absorption efficiency of structural component but, of course, says nothing about the efficiency of the structure in regards to other areas, such as resisting buckling, damping vibrations, or its ease of manufacture. It is one of several parameters that must be considered in automotive design.

Another important factor in the study of energy absorption for energy management capabilities is the shape of the crush load vs. crush length trace. Figure 1 shows an ideal crush load vs. crush length trace. As the crushing begins, the load quickly rises to a peak value, then drops off slightly and stays relatively constant. In this way the energy absorption is maximized for the length of crushed material. One does not want the initial peak load (F_{imax}) to be much greater than the average crush load (F_a),

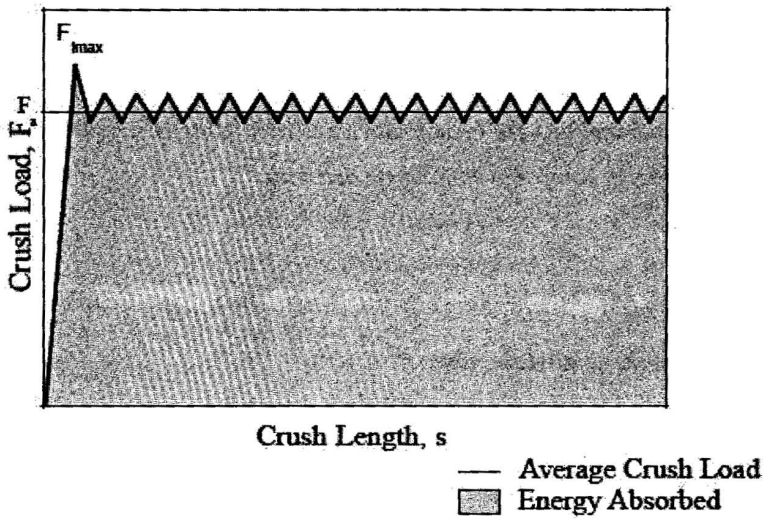

Figure 1: Ideal crush load vs. crush length

because large loads would be needed to initiate crushing, and the goal in energy management is to absorb all the energy without imparting large forces to the people involved. One measure that is used to characterize the shape of the trace is called the load ratio. The load ratio, which is defined as

$$\text{load ratio} = F_{imax}/F_a$$

is one metric that may be used as another important parameter for measuring crushing efficiency. Karbhari, et al. cites other sources that suggest that the load ratio should less that 1.25 [7]. The load ratio clearly cannot be the only measure used to determine that crush efficiency. A member could have an attractive load ratio but also have very low energy absorption. Catastrophic failures are clearly not acceptable for energy management.

2. BACKGROUND

The usage of fiber materials are often used to reduce the weight of structures [5]. In the automotive industry weight reduction is important because fuel consumption is directly related to vehicular weight. Federal regulations requiring increased fuel efficiency are forcing the industry to examine new light weight materials for major structural components. In addition, there is an increased concern for occupant safety during roadway accidents. Though active devices such as front, side, and knee airbags, and pop-out devices may be one solution, using the passive capacity of the structure is also attractive. Metals are currently used in car frames and integrated frame-body structures, and these and other metallic components are designed to passively absorb energy during accidents [6,8]. However, automotive manufacturers are moving toward nontraditional materials, and any new structural materials under consideration should be capable of participating in the energy absorption process associated with accidents. Recent work has shown that it is possible to use composite materials as both structural and energy absorbing members.

3. EXPERIMENTAL DEVELOPMENT

3.1 Specimens

Three parameters are considered in the experiment; geometry, fiber and densities. The fibers used were Empty Fruit Bunch (EFB) and Oil Palm Frond (OPF). In order to select the best form of fiber that would be put into the tubes, three type of fiber were tested; dry, added with water and added with urea formaldehyde. Figure 2 shows the typical Oil Palm Frond (OPF) fiber. Water was added to see if it can help the process of putting the fiber into the tubes so that the fiber will spread in the tube constantly. The two types of specimens then heated in the oven at about 12 hours.

Figure 2: The typical Oil Palm Frond (OPF) fiber

All specimens subjected to initial experimental works were into the length of 133 mm. Initial experimental works were done to select the best geometry and forms of fiber that will be put into the tubes. After selecting the proper combination between those two parameters, the real experimental work would be done. The length of the tube then changed to 250 mm and the forms of the fiber were decided to be dry at its own. The length was changed

because it is more clearer and easier to observe the mode of collapse of the tube, and the fiber forms was decided like that because based on the highest SEA of the tubes filled with dry EFB fiber. Figure 4 shows the cross section geometries of square and rectangular tubes. The fillet radius was 2.5 mm.

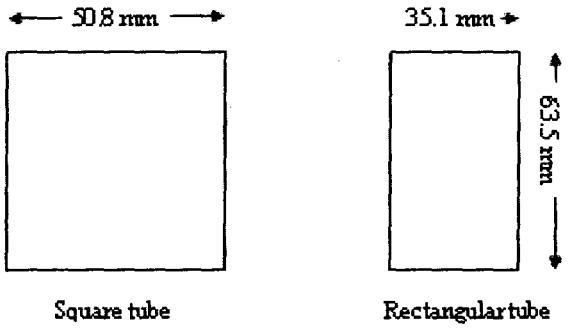

Figure 3: Cross section geometry of the tubes

In order to make sure that the comparison was reliable and acceptable the total circumferential length of the two cross section must be the same.

The initial densities of the fiber were chosen to be 150 kgm^{-3}, 200 kgm^{-3}, 250 kgm^{-3} and 300 kgm^{-3}. But for initial experimental works the initial densities were random ranging from 150 kgm^{-3} to 345 kgm^{-3}.

3.2 Cutting/labeling scheme

The tube name is a code that gives the cross-head speed, tube geometry, number of specimen and fiber type that filled into the tubes. The first character tells the loading rate of the cross-head speed: "5" for 5 mm/minute, "10" for 10 mm/minute and "20" for 20 mm/minute. Then, the second character tells the tube geometry: "S" for square cross-section, and "R" for rectangular cross-section. Next, the number, starting from "1001" and ended with "1018" indicates the number of the specimen. Type of fiber is indicated by its own initial. "EFB" is for Empty Fruit Bunch, "OPF" is for Oil Palm Frond and "E" is for empty. Lastly, the initial density of fiber that is put into the tubes is shown by "A", for 150kgm^{-3}, "B", for 200kgm^{-3}, "C" for 250kgm^{-3} and "D" for 300kgm^{-3}. A clear description of the specimen is shown in Table 1 below.

Code of specimen	Cross head speed (mm/min)	Tube geometry	Number of specimen	Type of fiber	Density of fiber (kgm^{-3})
5S1001E	5	Square	1001	Empty	Specimen were used to see if there is any significant effect by loading rate
5R1002E	5	Rectangular	1002	Empty	
20S1003E	20	Square	1003	Empty	
20R1004E	20	Rectangular	1004	Empty	

10S1005E	10	Square	1005	Empty	-
10R1006E	10	Rectangular	1006	Empty	-
10S1007EFBA	10	Square	1007	EFB	150
10R1008EFBA	10	Rectangular	1008	EFB	150
10S1009EFBB	10	Square	1009	EFB	200
10R1010EFBB	10	Rectangular	1010	EFB	200
10S1011EFBC	10	Square	1011	EFB	250
10R1012EFBC	10	Rectangular	1012	EFB	250
10S1013EFBD	10	Square	1013	EFB	300
10R1014EFBD	10	Rectangular	1014	EFB	300
10S1015OPFA	10	Square	1015	OPF	150
10R1016OPFA	10	Rectangular	1016	OPF	150
10S1017OPFB	10	Square	1017	OPF	200
10R1018OPFB	10	Rectangular	1018	OPF	200
10S1019OPFC	10	Square	1019	OPF	250
10R1020OPFC	10	Rectangular	1020	OPF	250
10S1021OPFD	10	Square	1021	OPF	300
10R1022OPFD	10	Rectangular	1022	OPF	300

Table 1: Codes details of specimens

3.3 Quasi-static testing

The quasi-static testing was performed at Structure and Material Lab II of Kolej Universiti Teknikal Kebangsaan Malaysia. The quasi-static test setup is shown by Figure 5. These tests were done on an Instron model 8858 displacement-control machine with a 300 kN load cell. The cross-head speed was set at 10 mm/minute. The specimen was placed on the stationary lower platen and it must be centered so that the load was effectively crushing the tube. The cross-head was then lowered until the upper platen was just touching the specimen. Using the software provided, then, balance load step was done to make sure that when the cross-head starting to crush the tube it is started from approximately 0 N. The cross-head was then set into motion and the load and cross-head displacement were recorded for each test. Some of the tests were recorded with a video camera.

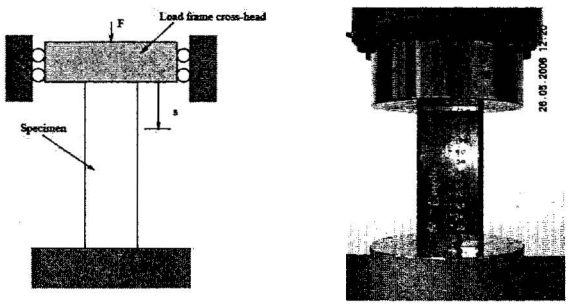

Figure 4: Schematic and picture of the quasi-static test setup

3.4 Specimen material analysis

Several measures were taken to determine the quality and consistency of the specimen. Inner and outer diameter (inner and outer square side lengths were measured for the tubes), length, and mass were measured for each specimen. Wall thickness measurements were also made for each specimen. The inner and outer side lengths were measured at two three locations on each of the tubes. Length was measured in three places for each tube and mass was measured twice. The wall thickness of the specimens was measured in four places on each end. The wall thickness was measured on each flat and each corner of each end of the specimen because the tubes were much thinner in the corners than on the flats. The side lengths were measured using calipers. The lengths of the tubes were measured with steel rulers. A micrometer was used to measure the wall thickness. The mass was determined using a Mettler PE 16 electronic scale.

3.5 Reduction of data

3.5.1 Calculating the Specific Energy Absorb (SEA) and Load ratio

The most important parameter that was determined from each crush test was the specific energy absorption (SEA). Energy is the product of the force and distance moved at that force level. The crush load, F, and crush length, s, obtained from the quasi-static tests are shown in Figure 5. The energy absorbed during crush, E, was then calculated by integrating under the crush load vs. crush distance curve,

$$E = \int_0^{s_f} F \cdot ds \,, \tag{1}$$

where s_ρ is the final crush length or locking strain point.

The average crush force was calculated continuously as the tube was crushed, as follows:

$$F_a = \frac{\int_0^s F \cdot ds}{s} \tag{2}$$

To calculate the load ratio, using Equation 2, the value of the crush load at the initial peak, F_{imax}, was divided by the average crush load,

$$load\ ratio = \frac{F_{imax}}{F_a} = \frac{F_{imax}}{\frac{\int_0^{s_f} F \cdot ds}{s_f}}. \tag{3}$$

To get the SEA, the energy absorbed during crush (until it reach locking strain) was divided by the mass of the crushed material, m_c. The crushed mass was found by the following:

$$m_c = m_l \cdot s_f \quad (4)$$

where m_l is the linear density or mass per unit length of the tube. The linear density was determined from the length and mass measurements from each specimen. The force and cross-head displacement (crush distance) were measured directly during the tests.

3.5.2 Calculating the energy absorbs

Before getting the SEA of the tubes, the energy absorb at locking must be calculated. Microcal Origin 5.0 software is used to get the energy absorbs. Firstly, the point of the locking strain must be identified. Refer to graph below; at the end of crushing test, there will be slightly a straight graph or line. By choosing the most stable and straight line, draw a straight line redundant at the straight line before. Then, using Microsoft Office Excel gets the regression line that will intercept with the other line. Referring to the interception point, then refer again to the displacement point at the axis below.

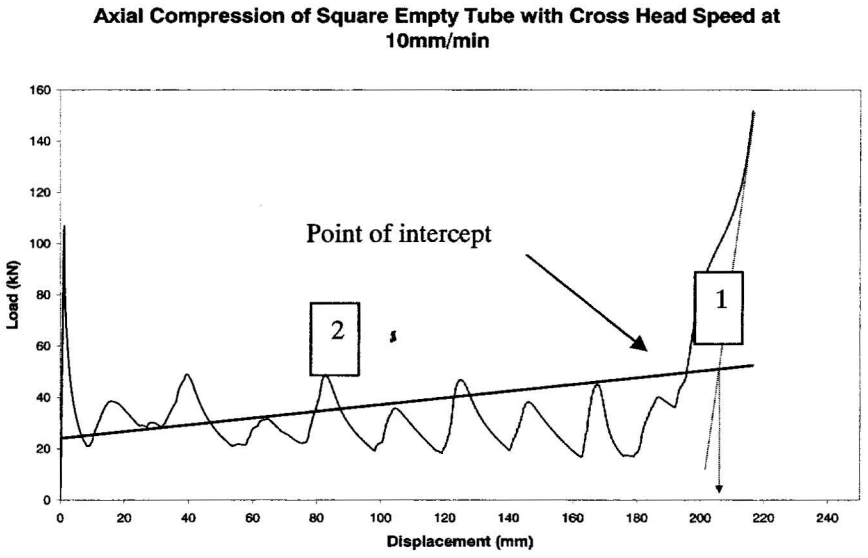

Figure 5: Two lines that will used to calculate the EA of the tubes; (1) line that is parallel to straight graph and (2) line is get from regression model of the graph

After obtaining the displacement point or known as locking strain point, refer back to the data regarding the locking strain point and then using Microcal Origin 5.0, integrate the graph. The energy absorbs then will be displayed by the software.

4. RESULT AND DISCUSSION

4.1 Crushing modes

There were several different modes of crush observed during the static crush tests. Almost all the tubes were crushed with diamond or multi-lobe mode. Some of them also buckle with mix mode. Mix mode deformation always happened at the end part of the tube. Depend on the geometry of the end part of the tube, the deformation can start either upper end or below end. But in some cases the deformation can start slightly at the centre part of the tube. This is either because the centre part of the tube is the weakest part or the end part was perfectly square that the centre of the tube becomes the concentrated place of the force.

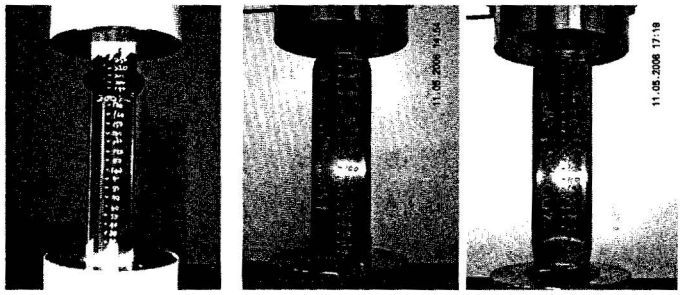

(i) (ii) (iii)

Figure 6: Deformation of the tube starts slightly at the centre (i), upper end part (ii) and lower end part (iii).

4.2 Quasi-static energy absorption characteristics of square tubes

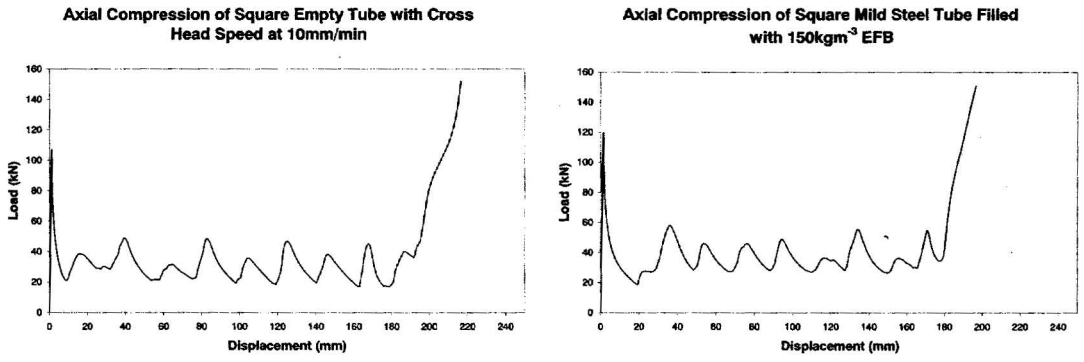

(i) (ii)

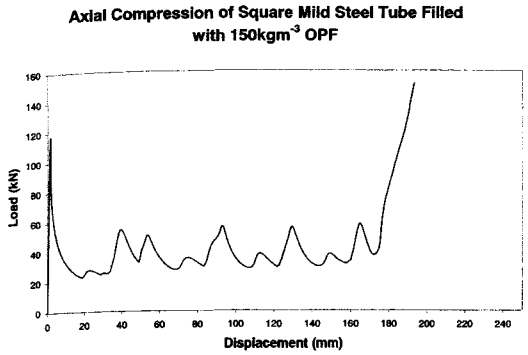

(iii)

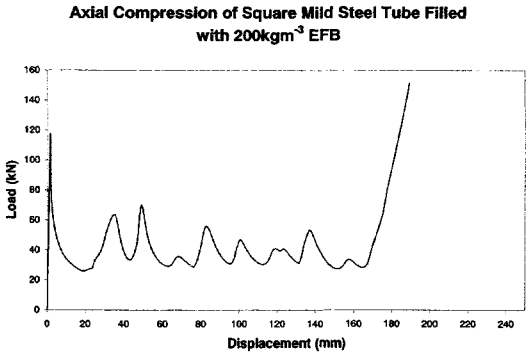

(iv)

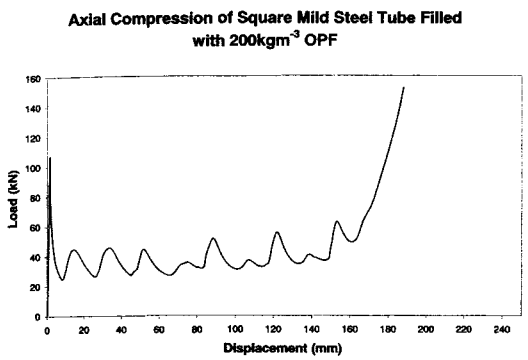

(v)

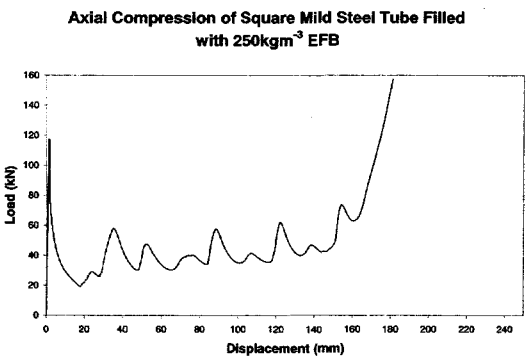

(vi)

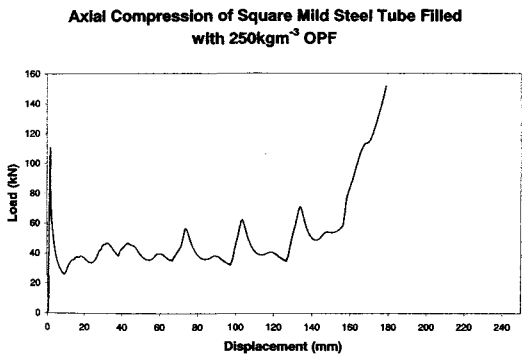

(vii)

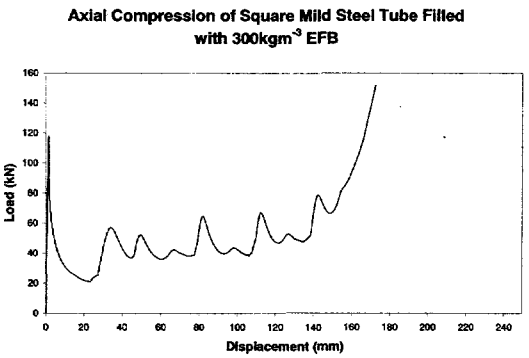

(viii)

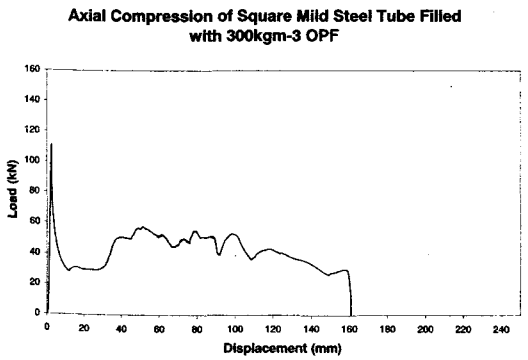

(xi)

Figure 7: Load vs. displacement curve for axial compression of square tubes. (i) 10S1005E (ii) 10S1007EFBA (iii) 10S1009EFBB (iv) 10S1011EFBC (v) 10S1013EFBD (vi) 10S1015OPFA (vii) 10S1017OPFB (viii) 10S1019OPFC (xi) 10S1021OPFD

The crush load vs. displacement traces for the quasi-static tests of the square mild steel tubes specimens are seen in Figure 7, All of the rectangular quasi-static specimens were crushed approximately to 150 kN load limit. It is seen that for this square tubes, most of the crush load vs. displacement traces approximately show a clear progressive shape of fluctuation except for. The 300 kgm^{-3} OPF specimen deforms in Euler buckling mode and before that it actually show two lobes in diamond mode. All of the curves show the initial peaks above 100 kN and slightly narrow valley-to-peak variation. Almost all of the peaks and valley of curve starting from initial to the last show a sharp fluctuation. This phenomenon is actually expected to occur because the geometrical effect of the tubes.

The SEA for empty square tubes shows the best when among filled tubes. When only this characteristic was considered, the objectives seem not achieved. Load ratio for empty tubes is very high and exceeded tremendously and also cannot be considered as a good energy absorption device. The SEA for filled tubes is lower than the empty tubes. Load ratio for filled tubes is better that the empty tubes but cannot be considered as acceptable because it is exceeded far from 1.25 [7]. It is shown that the best combination between SEA and load ratio for crushed square tubes is 10S1019OPFC.

Code of specimen	Energy absorb at locking strain, E_l (Nm)	Mass of specimen, m (kg)	Specific energy absorb, E_s (J/kg)	Load ratio
10S1005E	6.86E+03	0.53034	1.29E+04	3.15
10S1007EFBA	6.50E+03	0.62035	1.05E+04	3.20
10S1009EFBB	6.54E+03	0.60872	1.08E+04	3.10
10S1011EFBC	6.69E+03	0.63236	1.06E+04	2.98
10S1013EFBD	6.63E+03	0.63782	1.04E+04	2.74
10S1015OPFA	6.95E+03	0.66014	1.05E+04	2.73
10S1017OPFB	6.82E+03	0.66106	1.03E+04	2.56
10S1019OPFC	7.44E+03	0.69046	1.08E+04	2.47
10S1021OPFD	~	~	~	~

Table 2: *SEA* for square mild steel tubes subject to axial loading.

4.3 Quasi-static energy absorption characteristics of rectangular tubes

Axial Compression of Rectangular Empty Tube with Cross Head Speed at 10mm/min

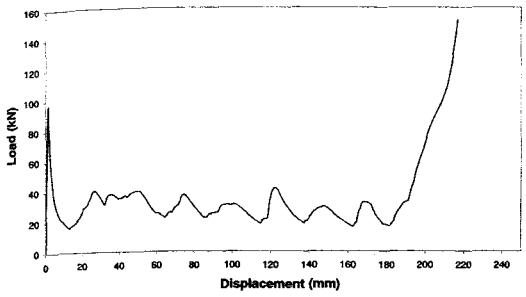

(i)

Axial Compresssion of Rectangular Mild Steel Tube Filled with 150kgm^{-3} EFB

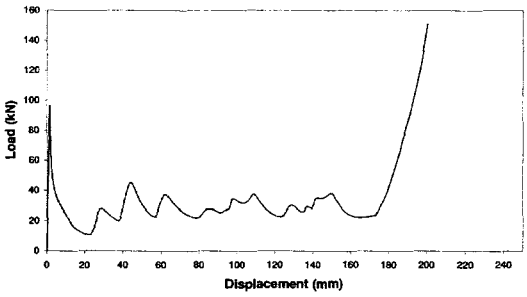

(ii)

Axial Compression of Rectangular Mild Steel Tube Filled with 150kgm^{-3} OPF

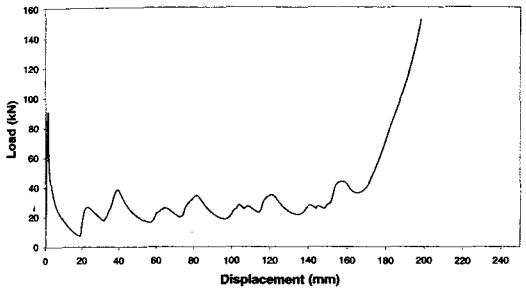

(iii)

Axial Compression of Rectangular Mild Steel Tube Filled with 200kgm^{-3} EFB

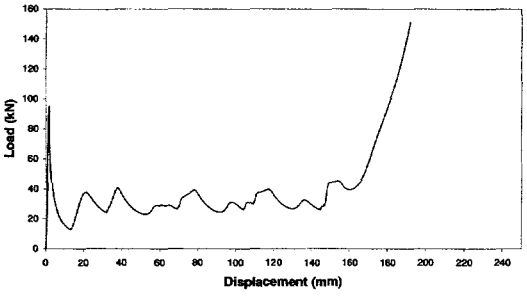

(iv)

Axial Compression of Rectangular Mild Steel Tube Filled with 200kgm^{-3} OPF

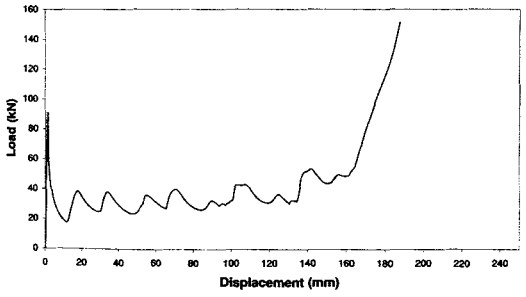

(v)

Axial Compression for Rectangular Mild Steel Tube Filled with 250kgm^{-3} EFB

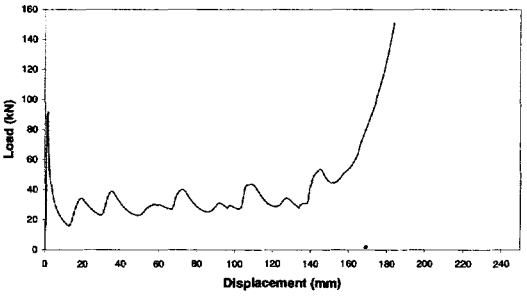

(vi)

Axial Compression for Square Mild Steel Tube Filled with 250kgm^{-3} OPF

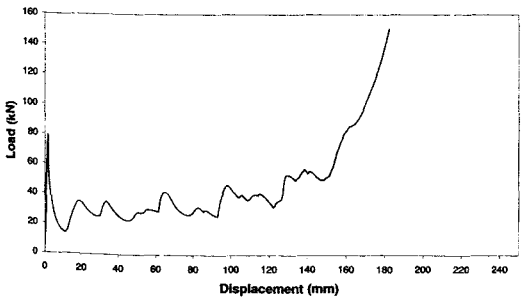

(vii)

Axial Compression of Rectangular Mild Steel Tube Filled with 300kgm^{-3} EFB

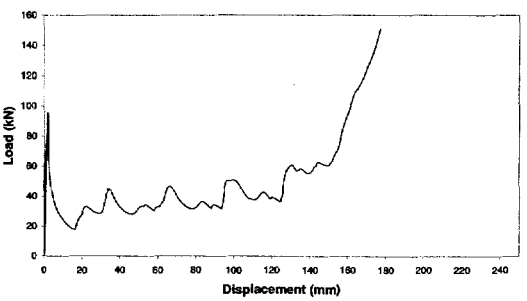

(viii)

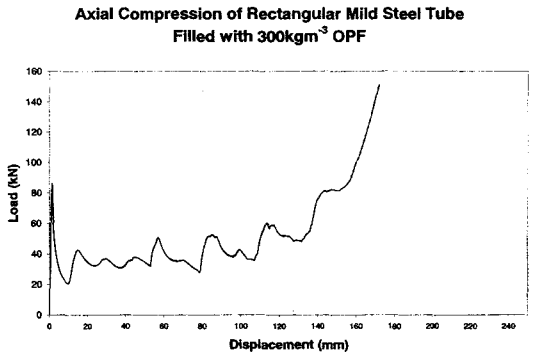

(xi)

Figure 8: Load vs. displacement curve for axial compression of rectangular tubes. (i) 10R1006E (ii) 10R1008EFBA (iii) 10R1010EFBB (iv) 10R1012EFBC (v) 10R1014EFBD (vi) 10R1016OPFA (vii) 10R1018OPFB (viii) 10R1020OPFC (xi) 10R1022OPFD

The crush load vs. displacement traces for the quasi-static tests of the rectangular mild steel tubes specimens are seen in Figure 8, All of the rectangular quasi-static specimens were crushed approximately to 150 kN load limit. It is seen that for this rectangular tubes, most of the crush load vs. displacement traces approximately show a stable and progressive shape of fluctuation. All of the curves show the initial peaks below 100 kN and large valley-to-peak or smooth variation and that is actually a very good shape of curve for energy absorption characteristics so that the energy can be absorb higher.

The SEA for empty rectangular tubes shows are higher than filled tubes. Load ratio for empty tubes is very high and exceeded tremendously and also cannot be considered as a good energy absorption device. The SEA for filled tubes is lower than the empty tubes. The load ratio for 10R1008EFBA and 10R1022OPFD tubes are almost the same with suggested by Karbhari, et al. and can be considered as acceptable because it is approximately not far from 1.25 [7]. It is shown that the best combination between SEA and load ratio for crushed square tubes is 10R1022OPFD.

Code of specimen	Energy absorb at locking strain, E_l (Nm)	Mass of specimen, m (kg)	Specific energy absorb, E_s (J/kg)	Load ratio
10R1006E	6.16E+03	0.55883	1.10E+04	3.17
10R1008EFBA	5.32E+03	0.6385	8.34E+03	1.64
10R1010EFBB	5.02E+03	0.6384	7.87E+03	3.21
10R1012EFBC	5.83E+03	0.66443	8.78E+03	2.84
10R1014EFBD	6.38E+03	0.66521	9.59E+03	2.45
10R1016OPFA	5.84E+03	0.69168	8.44E+03	2.63
10R1018OPFB	6.53E+03	0.69139	9.44E+03	2.01
10R1020OPFC	6.83E+03	0.71803	9.52E+03	2.25
10R1022OPFD	7.17E+03	0.71756	9.99E+03	1.89

Table 3: *SEA* for rectangular mild steel tubes subject to axial loading.

4.4 Geometry effect on energy absorption characteristics of tubes

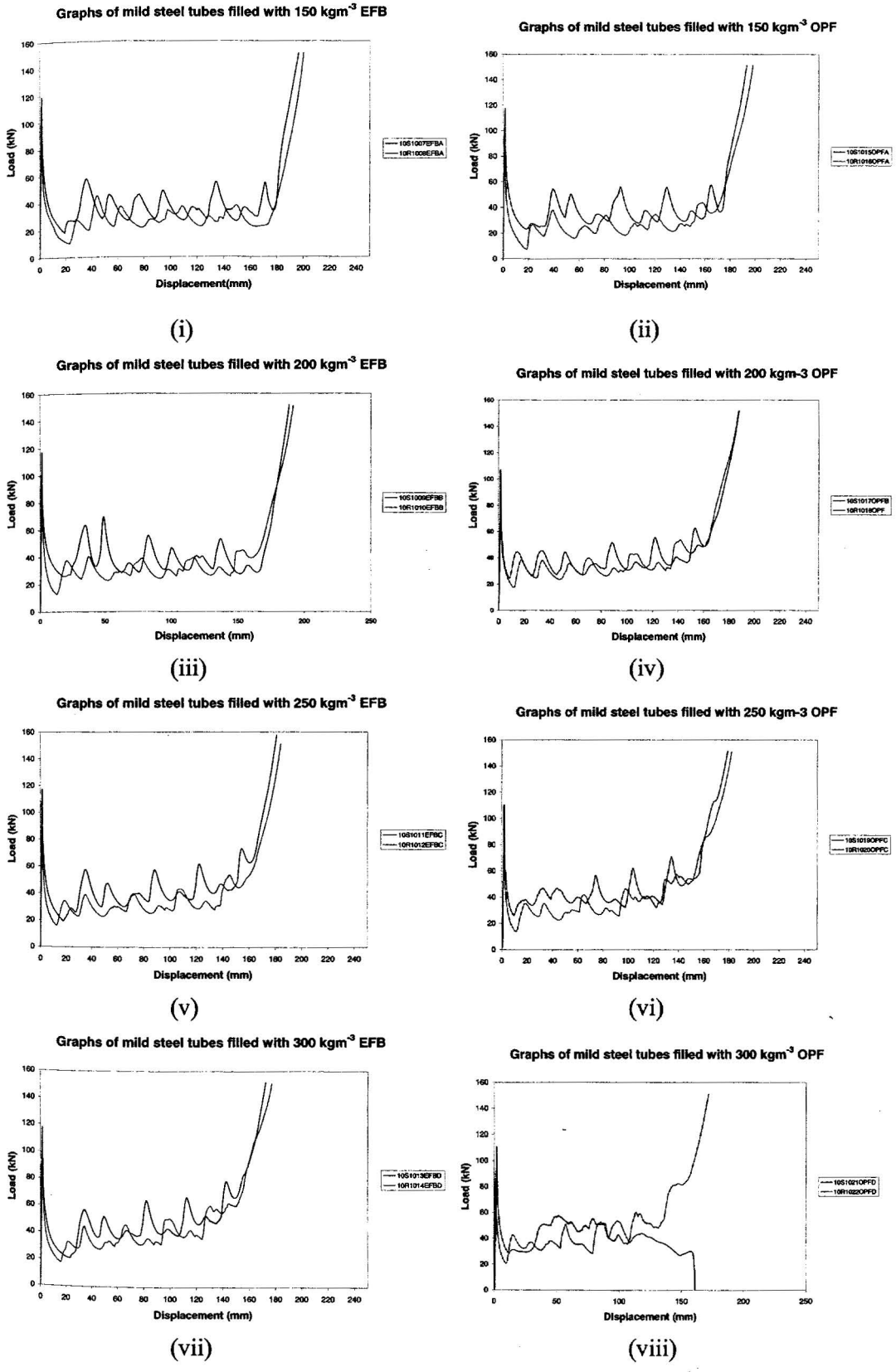

Figure 9: Combination of load-displacement curve between square and rectangular mild steel tubes filled with EFB and OPF. (i) Combination of 10S1007EFBA and 10R1008EFBA (ii) Combination of 10S1009EFBB and

10R1010EFBB (iii) Combination of 10S1011EFBC and 10R1012EFBC (iv) Combination of 10S1013EFBD and 10R1014EFBD (v) Combination of 10S1015OPFA and 10R1016OPFA (vi) Combination of 10S1017OPFB and 10R1018OPFB (vii) Combination of 10S1019OPFC and 10R1020OPFC (viii) Combination of 10S1021OPFD and 10R1020OPFD.

The combination of load-displacement curve between square and rectangular mild steel tubes filled with EFB and OPF are shown in Figure 9. All of the specimens were crushed approximately up to 150 kN load limit except for 10S1021OPFD because it deform in Euler buckling mode and jump out of the load frame before reaching the load limit. It seems that crush load vs. displacement traces for square tubes show a sharp and stable shape of fluctuation than rectangular tubes. Initials peaks for the square tubes curves always exceeded 100 kN and rectangular tubes are below 100 kN. Other than that, almost all the peaks and valleys of square tubes are higher than rectangular tubes. Rectangular tubes peaks and valleys are smoother than those of square tubes and this is a good characteristic for energy absorption device. Sharp peaks means there is a sudden change in load that will create inertia effect and it will also influence the passenger to jump out of the compartment.

The SEA for square tubes is better that rectangular tube. But load ratio for rectangular tubes is lower that those of square tubes. As a result, rectangular tubes show a better combination between SEA and load ratio to be considered as a good energy absorption device.

4.5 Type of fiber effect on energy absorption characteristics of tubes

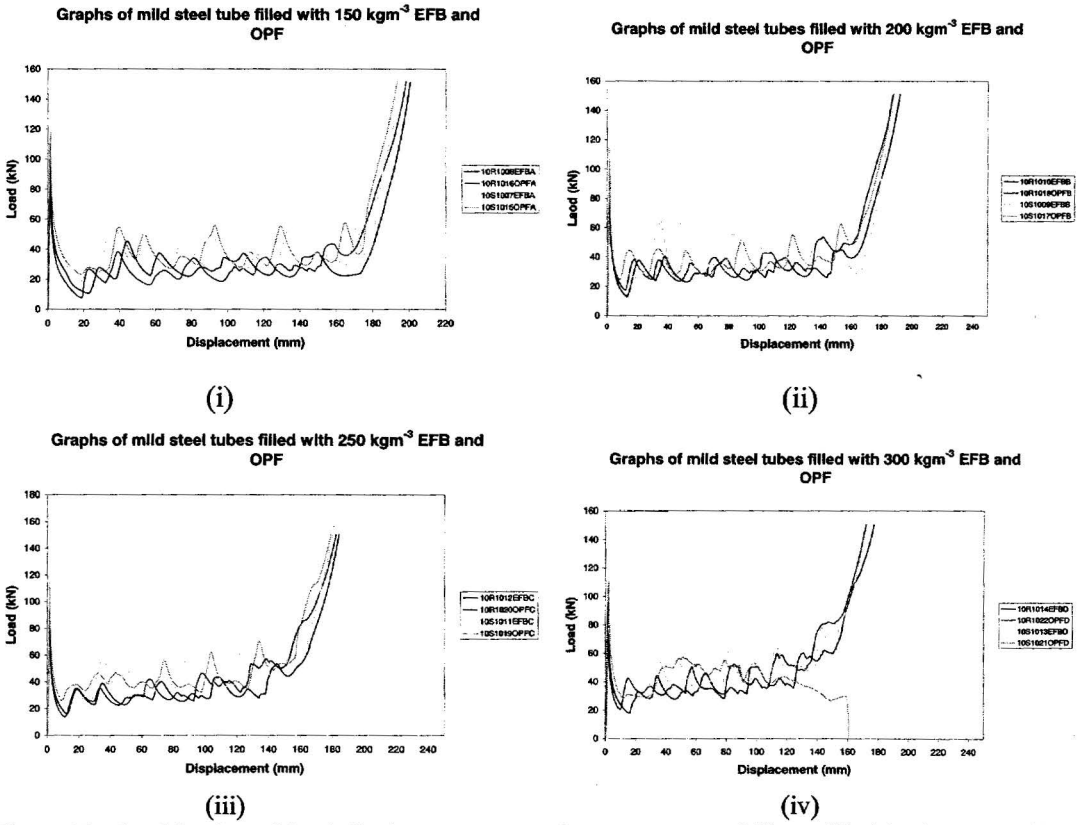

Figure 10: Combination of load-displacement curve between types of fibers filled in the tubes. (i) Combination of 150kgm^{-3} density fiber filled in the tubes. (ii) Combination of 200kgm^{-3} density fiber filled in the tubes. (iii)

Combination of 250kgm^{-3} density fiber filled in the tubes. (iv) Combination of 300kgm^{-3} density fiber filled in the tubes.

The crush loads vs. displacement traces between types of fibers filled in the tubes are shown in Figure 10. The effect of fiber that filled in the tubes is actually having close relation with the density of it. When the density of the fiber that crushed in the tubes comes into some level, and have a close contact between them and the tubes then the effect of it will occur. The microstructure of the fiber is the main factors that will effect the energy absorb by the tubes. Referring to the load-displacement curve above, the effect of fiber start at almost half of the crush length of the tubes. One of the most significant effect is that the peaks and valleys become smaller and smoother.

Actually the effect of fibers to the energy absorb, in particular, is really difficult to see unless it involved large scale of specimen. The effect of fiber is difficult to see because the effect of tube geometry has made it disappear. Almost all of *SEA* of OPF is higher from EFB.

4.6 Initial density effect on energy absorption characteristics of tubes

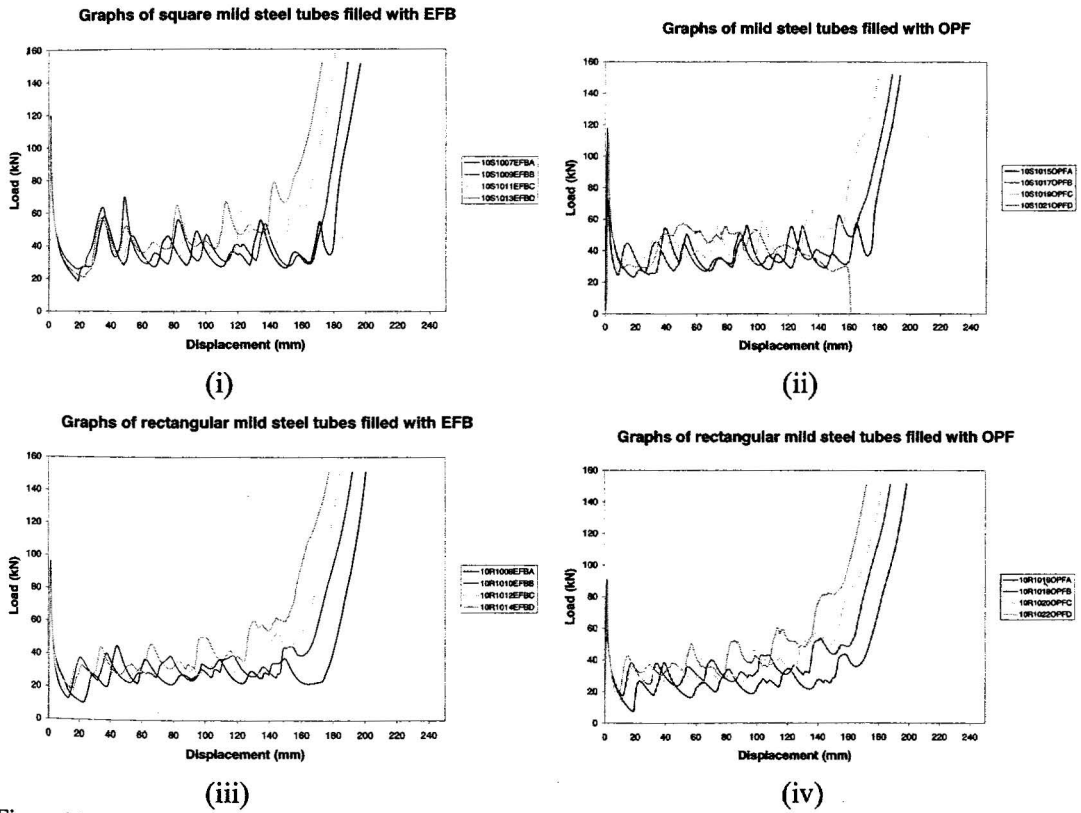

Figure11: Combination of load-displacement curve between initial densities of fiber filled in the tubes. (i) Combination of square tubes filled with EFB. (ii) Combination of square tubes filled with OPF (iii) Combination of rectangular tubes filled with EFB (iv) Combination of rectangular tubes filled with OPF.

The combination of load-displacement curve between initial densities of fiber filled in the tubes is shown in Figure [11], All of the specimens were crushed approximately to 150 kN load limit but the crush length is different depend on the densities of the fiber filled in the tube. When the initial densities become higher, the

crush length will become shorter. It is mean that the densification effect had occurred through the compression of the tubes. Peaks and valleys will become higher and different from the beginning till the end of compression. Effect of densification has made square tube filled with 300 kgm^{-3} OPF deform in Euler buckling mode. It jumps out of the load frame.

Almost all SEA value of the specimens directly proportional to the initial density of fiber filled in the tubes except to EFB filled in the square tubes. Load ratio seems to be unstable and difficult to be predicted. The best load ratio is 1.64, and it is rectangular tubes filled with 150 kgm^{-3} EFB.

5. CONCLUSION

There are three parameters; geometry, type of fiber and initial density of fiber filled, that were used in the experimental works. The main objectives were to compare how the energy absorption characteristics were changed by varying these several parameters:

The specimens with square tubes show a stable and progressive fluctuation of load-displacement curve while rectangular tubes show a smooth and slightly unstable curve. Considering only by geometry effect, SEA for square tubes is higher at almost all specimens comparing to rectangular tubes. But, load ratio for rectangular tubes is likely to be very appropriate to act as a good energy absorption device. The highest SEA of all tubes is square empty tube with 1.29E+04 J.

Type of fiber does not show any significant effect to the SEA. But in almost all condition, OPF show a better value between them except for OPF with 200 kgm^{-3} filled in square tube. Microstructure seems not really effect the SEA for both type of tubes.

Densities of fiber show a great effect to EA but not SEA of all tubes. The effects always occur at the half crush length. It helps to increase the energy absorb by co-operate with the tube itself to act as energy absorption part especially when the densification effect become higher. When the initial densities are higher then the crush length will become shorter. In this experiment, square tube filled with 200 kgm^{-3} EFB and 250 kgm^{-3} OPF show great value of SAE.

By considering all factors, rectangular tube filled with OPF with 300 kgm^{-3} density is the best of all specimens' tests. It absorbs 9.99E+03 J/kg and has a good load ratio of 1.89.

REFERENCES

[1] Johnson W, Ried SR. Metallic energy dissipating systems. Appl Mech Rev 1978;31:277.

[2] Jones N, Wierzbicki T. Structural crashworthiness. London: Butterworths, 1983

[3] Jones N, Wierzbicki T. Structural crashworthiness and failure. London: Elsevier Applied Science, 1993

[4] Morton J. Structural impact and crashworthiness. London: Elsevier Applied Science, 1984.

[5] Farley GL, Jones RM. Crushing characteristics of continuous fiber-reinforced composite tubes. J Compos Mater 1992;26:37.

[6] Thornton P. Energy absorption by foam filled structures. SAE paper 800081, 1980.

[7] Karbhari, Vistap M., Falzon, Paul J., and Herzberg, "Energy absorption characteristics of hybrid braided composite tubes," Journal of Composite Material, Vol. 31, No 12.1997, pp. 1165-1186.

[8] Lampinen BE, Jeryan RA. Effectiveness of polyurethane foam in energy absorption structures. SAE paper 820494, 1982.

[9] Reid SR, Reddy TY, Gray MD. Static and dynamic axial crushing of foam-filled sheet metal tubes. Int. J Mech Sci 1986;28(5)

[10] Abromowicz W, Wierzbicki T. Axial crushing of foam-filled columns. Int. J Mech Sci 1988;30(3/4):263

[11] Ashby MF. The mechanical properties of cellular solids. Met Trans 1983;14A:1755-69.

[12] Gibson LJ, Ashby MF. Cellular solids: structure and properties. Oxford: Pergamon Press, 1988.

[13] Hanssen AG, Langesh M, Hopperstad OS. Static crushing of square aluminium extrusions with aluminium foam filler. Int. J Mech Sci 1999;41;967-93.

[14] Reddy TY, Al-Hassani STS. Axial crushing of wood-filled square metal tubes. Int. J Mech Sci 1993;35(3/4):231-46.

[15] Singace AA. Analysis of axially crushed tubes deforming in multi-lobe mode. Int. J Mech Sci 1999;41(7):865-90.

[16] Johnson W, Soden PD, Al-Hassani STS. Inextensional collapse of thin-walled tubes under axial compression. J Strain Anal 1977;12(4):317.

[17] Singace AA, El-Sobky H, Reddy TY. On the eccentricity factor in the progressive crushing of tubes. Int J Solids Struct 1995;32;3589-602.